

## Celiac and superior mesenteric ganglia removal improves glucose tolerance and reduces pancreas islet size

Shanshan Xu<sup>a,d</sup>, Misaki Inoue<sup>a</sup>, Yuki Yoshimura<sup>a</sup>, Kunio Kondoh<sup>a</sup>, Keiji Naruse<sup>b,d</sup>, Takeshi Y. Hiyama<sup>a,c,\*</sup>

<sup>a</sup> Department of Integrative Physiology, Tottori University Graduate School and Faculty of Medicine, Yonago, Japan

<sup>b</sup> Department of Cardiovascular Physiology, Graduate School of Medicine, Dentistry and Pharmaceutical Sciences, Okayama University, Okayama, Japan

<sup>c</sup> International Platform for Dryland Research and Education, Tottori University, Tottori, Japan

<sup>d</sup> Department of Cellular Physiology, Graduate School of Medicine, Dentistry and Pharmaceutical Sciences, Okayama University, Okayama, Japan

### ARTICLE INFO

#### Keywords:

Celiac ganglion  
Superior mesenteric ganglion  
Pancreas islet

### ABSTRACT

The sympathetic nervous system is crucial for the regulation of visceral organ function. For instance, the activation of the sympathetic nervous system promotes glycogenolysis in the liver and modulates glucagon and insulin release from the pancreas, thereby raising blood glucose levels. A decrease in sympathetic nerve activity has the opposite effect. Although such acute effects of sympathetic activity changes have been studied, their long-term outcomes have not been previously examined. In this study, we removed the celiac/superior mesenteric ganglia, where sympathetic postganglionic neurons innervating pancreas and liver locate, and examined its effects on glucose homeostasis and islet size several weeks after surgery. Consistent with the reduction in gluconeogenesis, glucose tolerance improved in gangliectomized mice. However, contrary to our expectation that the inhibition of pancreatic function by sympathetic nerves would be relieved with gangliectomy, insulin or C-peptide release did not increase. Examining the size distribution of pancreatic islets, we identified that the gangliectomy led to a size reduction in large islets and a decrease in the proportion of  $\alpha$  and  $\beta$  cells within each islet, as analyzed by immunostaining for insulin and glucagon, respectively. These results indicate that the absence of sympathetic nerve activity reduces the size of the pancreatic islets within a few weeks to reinstate the homeostatic mechanism of blood glucose levels.

### 1. Introduction

The abdominal organs receive sympathetic postganglionic fibers from the celiac plexus, which is a complex integrative center of autonomic nerve fibers [1]. Tracing studies have revealed projections from the postganglionic neurons in the celiac and superior mesenteric ganglia (CG/SMG) of the celiac plexus to several organs, including the pancreas and liver [1–3]. Recent three-dimensional imaging studies have demonstrated dense sympathetic innervation in pancreatic islets, suggesting that the nerves directly modulate islet  $\alpha$  and  $\beta$  cells function in response to internal and external stimuli [4–7].

The  $\alpha$  and  $\beta$  cells of pancreatic islets secrete the pancreatic hormones glucagon and insulin, respectively [7]. Glucagon promotes glycogenolysis in the liver, leading to the breakdown of glycogen stores into glucose, which is then released into the bloodstream [8]. Conversely, insulin acts directly on the liver to inhibit glycogenolysis, facilitates the

uptake of glucose into nearly all organ cells, and promotes glycogen synthesis and storage in the liver and muscles [9]. Electrical stimulation experiments on visceral nerves suggest that the activation of the sympathetic nervous system increases glucagon and inhibits insulin secretion, leading to increased blood glucose levels [7]. However, a recent study demonstrated that the specific activation of sympathetic efferent neurons innervating the pancreas did not change plasma insulin or glucagon levels, prompting us to reconsider the role of sympathetic nerves in the pancreas [10].

Although many studies have focused on the acute effects of sympathetic activity modulations on pancreatic function, the impact of sympathetic nervous system alterations over several weeks has not been analyzed. In this study, we investigated the impact of diminished sympathetic nervous function over a few weeks by removing CG/SMG (CGX). Our findings revealed a shift in the distribution of pancreatic islet sizes towards small dimensions, accompanied by a decrease in the

\* Corresponding author at: Department of Integrative Physiology, Tottori University Graduate School and Faculty of Medicine, Yonago, Japan.

E-mail address: [hiyama@tottori-u.ac.jp](mailto:hiyama@tottori-u.ac.jp) (T.Y. Hiyama).

<https://doi.org/10.1016/j.neulet.2024.137919>

Received 31 May 2024; Received in revised form 16 July 2024; Accepted 28 July 2024

Available online 30 July 2024

0304-3940/© 2024 The Authors. Published by Elsevier B.V. This is an open access article under the CC BY license (<http://creativecommons.org/licenses/by/4.0/>).

proportion of  $\alpha$  and  $\beta$  cells per islet. These results suggested that sympathetic nerves play a crucial role in the sustained maintenance of pancreatic function.

## 2. Materials and methods

### 2.1. Animals

All animal experiments were performed according to protocols approved by the Animal Care and Use Committee of Tottori University (approval number 23-Y-45). Adult male wild-type C57BL/6J mice from CLEA were housed in separate cages for more than 2 weeks and managed under regular conditions (room temperature  $23 \pm 1$  °C and a 12-hour light/dark cycle on am 9:00-to-21:00 light cycle) with water and mouse chow available *ad libitum* (Rodent Diet CE-2, CLEA Japan).

### 2.2. Retrograde labelling

The mice were anesthetized with medetomidine (Domitor; Nippon Zenyaku Kogyo, Fukushima, Japan), midazolam (SANDOZ; SANDOZ, Tokyo, Japan), and butorphanol (Vetorphale; Meiji Seika Pharma, Tokyo, Japan) at doses of 0.3, 4, and 5 mg/kg body weight [bw], respectively [11]. The incision area was shaved and prepared using an ethanol scrub. Following laparotomy, the head and tail of the pancreas were identified as adjacent to the stomach and spleen. AAV-CAG-tdTomato (Addgene # 59462-AAVrg at titer  $\geq 7 \times 10^{12}$  vg/mL) was injected at eight sites per pancreas to be evenly administered throughout the entire organ. Using heat-pulled glass capillary tubes, a total of 4  $\mu$ L solution was injected at a rate of 250 nL/min, carefully avoiding damage to the blood vessels. Five minutes after each injection, the viscera were rinsed with sterile saline to reduce the possibility that a small amount of leaked virus infects the other tissues than pancreas. Then, the muscle and skin were sutured. The mice were allowed to recover for 4 weeks with free access to water and food. After being anesthetized again, mice were transcardially perfused with phosphate buffered saline (PBS), followed by fixation with 4 % paraformaldehyde (PFA) in PBS. The CG-SMG was excised for whole-mount observation using a confocal microscope with a tile function (LSM900, Zeiss, Jena, Germany).

### 2.3. CGX and sham surgery

All sham and CGX surgeries were performed on mice aged 12–16 weeks. Surgery was performed under anesthesia as described previously. The body temperature of the mice was maintained using a heating mat throughout the surgery. The CG-SMG was localized following the method described [12]. Visible nerves near the main vessels (eg. aorta, superior mesenteric artery, and celiac artery) were stripped and removed as completely as possible. The abdomen was closed in two layers using interrupted sutures. Mice were administered atipamezole 0.75 mg/kg bw (Antisedan, Zenoaq, Fukushima, Japan) to counteract the effects of anesthesia. For the sham surgery, the ganglion was exposed but not otherwise disturbed. All functional analyses were performed 2–8 weeks following the surgery.

### 2.4. Intraperitoneal (ip) glucose tolerance test (ipGTT) and ip pyruvate tolerance test (ipPTT)

Before the ipGTT and ipPTT, the mice were habituated to restraint for 1 min per day for 5 consecutive days. The mice were fasted overnight from 18:00 to 10:00 the following day with unrestricted access to water. Glucose for the ipGTT (2 g/kg bw) or sodium pyruvate for the ipPTT (2 g/kg bw) was delivered *via* ip injection. Blood glucose levels in the tail vein were monitored using a glucometer (Antsense DUO, HORIBA, Kyoto, Japan).

### 2.5. Intraperitoneal insulin tolerance test (ipITT)

Before ipITT, the mice were habituated to restraint for 1 min/day for 5 consecutive days. The mice were fasted for 2 h from 10:00 to 12:00, and 1.7 U/kg bw insulin (I9278; Merck, Darmstadt, Germany) was administered *via* ip injection. The blood glucose levels in the tail vein were monitored using a glucometer.

### 2.6. Insulin, C-peptide, and glucagon enzyme-linked immunosorbent assay (ELISA)

Plasma insulin, C-peptide, and glucagon levels were assessed using commercial ELISA kits (LBIS Mouse Insulin ELISA Kit U-type, 633–03411, Fujifilm, Tokyo, Japan; LBIS Mouse C-peptide ELISA Kit U-type, 631–07231, Fujifilm; Mercodia Glucagon ELISA 10  $\mu$ L, 10–1281-01, Mercodia, Uppsala, Sweden). During ipGTT or ipITT, 30–40  $\mu$ L or 70–80  $\mu$ L of blood was collected from the tail vein at various time points using hematocrit capillaries (9100275, Hirschmann Laborgeräte, Eberstadt, Germany). The blood was then transferred to a 0.5-mL tube coated with 1  $\mu$ L 1000 U/mL heparin-Na in 0.5 M ethylenediaminetetraacetic acid and 1  $\mu$ L aprotinin (O18–18111, WAKO, Osaka, Japan) and kept on ice. Plasma was subsequently separated by centrifugation (1,200 g for 15 min) and stored at  $-80$  °C. Blood (30–40  $\mu$ L) for 10  $\mu$ L plasma was used for insulin measurement, whereas and blood (70–80  $\mu$ L) for 20  $\mu$ L was used for plasma for C-peptide and glucagon measurement.

### 2.7. Immunofluorescence staining

All histological analyses were conducted 4–5 weeks after the surgery. Immunofluorescence staining was performed as described previously [13]. Briefly, anesthetized mice were perfused with PBS, followed by 4 % PFA in PBS. The pancreas or CG-SMG were dissected and post-fixed for 4 h (CG-SMG) or overnight (pancreas) in 4 % PFA in PBS at 4 °C. They were then incubated overnight at 4 °C in 30 % sucrose in PBS. Tissues were sliced at a thickness of 20  $\mu$ m using a freezing microtome (Leica, Germany). The slices were blocked with blocking solution (5 % bovine serum albumin (BSA), 0.1 % Triton X-100 in PBS) at room temperature (RT) for 1 h, followed by incubation with primary antibody (Chicken anti-tyrosine hydroxylase (TH), 1:500, ab76442, Abcam, Cambridge, UK; Guinea pig anti-insulin, 1:50, GTX27842, GeneTex, Irvine, CA; Rabbit anti-glucagon, 1:1000, ab92517, Abcam) in primary dilution buffer (1 % BSA, 0.3 % Triton X-100 in PBS) at 4 °C overnight. After washing four times for 5 min with PBS at RT, the samples were incubated with secondary antibodies (Donkey anti-rabbit Alexa594, 1:500, a21207, Invitrogen, Waltham, MA; Donkey anti-chicken Alexa488, 1:250, 703-545-155, Jackson ImmunoResearch, West Grove, PA; donkey anti-guinea pig Alexa594, 1:500, 706-585-148, Jackson ImmunoResearch; donkey anti-rabbit Alexa 648, 1:500, ab150075, Abcam) in blocking solution at RT for 2 h. After washing four times for 5 min with PBS at RT, Fluoromount-G mounting medium (with 4',6-diamidino-2-phenylindole [DAPI]) (00-4959-52, Invitrogen) was utilized to mount the slides.

### 2.8. Image capture and quantification analysis

Microscopic images were captured using an LSM900 confocal microscope (Zeiss) with ZEN imaging software (Zeiss). The entire tissue section was captured using a 10x lens with a tile function in two channels (DAPI and 647). Subsequently, individual islet images were captured using a 20x lens with a z-stack function in four fluorescent channels (488, 594, and 647 DAPI). Quantitative analysis of cellular composition, including islet area, TH,  $\beta$ , and  $\alpha$  cell area, was conducted using ImageJ software (<https://imagej.net/ij/>). Initially, merged images from the four fluorescent channels were employed to manually delineate the boundaries of each islet. Moreover, regions of interest (ROIs) were recorded and stored in the ROI manager to demonstrate the islet area.

Because TH is also expressed in pancreatic acinar cells and islet  $\beta$  cells [14], the TH-positive cell bodies were manually excluded from the TH area measurement for the assessment of sympathetic nerve innervation. Subsequently, single-channel images were converted to eight-bit masks and subjected to thresholding to measure the area of TH,  $\beta$ , and  $\alpha$  cell areas, utilizing the previously recorded ROIs.

## 2.9. Statistical analysis

Testing groups were balanced by age and genotype, and the randomization of experimental groups was not performed. No statistical methods were used to predetermine sample sizes. All statistical analyses were performed using GraphPad Prism software (GraphPad Software, Boston, MA, USA). The normality of the data was initially tested by the Shapiro-Wilk test. TH area per islet size of each mouse, plasma glucagon levels after overnight fasting, islet density, and islet area per pancreas area were analyzed using unpaired t-tests. The TH/insulin/glucagon area per islet size was compared using the Mann-Whitney *U* test. The ipGTT, ipITT and ipPTT time courses were analyzed using repeated measures and two-way analysis of variance with post-hoc Sidak's multiple comparisons test. Plasma glucagon levels during ipITT was analyzed using mixed-effects analysis. Percentage fractions of different-size islets in Fig. 3B were compared between sham and CGX using Pearson's Chi-squared test.

## 3. Results

### 3.1. CGX drastically reduces islet sympathetic innervation

To trace the neurons directly projecting to the pancreas, we injected AAVrg-CAG-tdTomato, an adeno-associated virus with a retrograde serotype (AAVrg), into the pancreas. Consistent with previous studies indicating that the neural innervation of the pancreas primarily originates from the CG-SMG [2], the expression of tdTomato, a red fluorescent protein, was observed in many CG-SMG neurons (Fig. 1A). As expected, after the CG-SMG removal (CGX) (Fig. 1B), sympathetic nerves detected by immunohistochemical staining of TH in islet significantly decreased in each mouse and each islet (Fig. 1C-E).

### 3.2. CGX improves glucose tolerance by reducing glucogenesis in the liver

After a recovery period of more than 2 weeks post-surgery, we examined whether the long-term absence of sympathetic innervation altered the regulation of glucose homeostasis by performing an ipGTT after overnight fasting (Fig. 2A). Pre-dose basal blood glucose levels did not demonstrate any statistically significant differences between the sham and CGX groups (0 min). Blood glucose levels after ip glucose dosing in the CGX group were significantly lower than those in the control sham group at 15, 30, 60, and 90 min, indicating that the CGX group exhibited improved glucose tolerance compared with that in the sham group. The improvement in glucose tolerance by CGX suggests at least two underlying mechanisms: the first is a reduction in the suppressive effect of sympathetic nerves on insulin release in the pancreas and the second is a reduction in sympathetic nerve-dependent

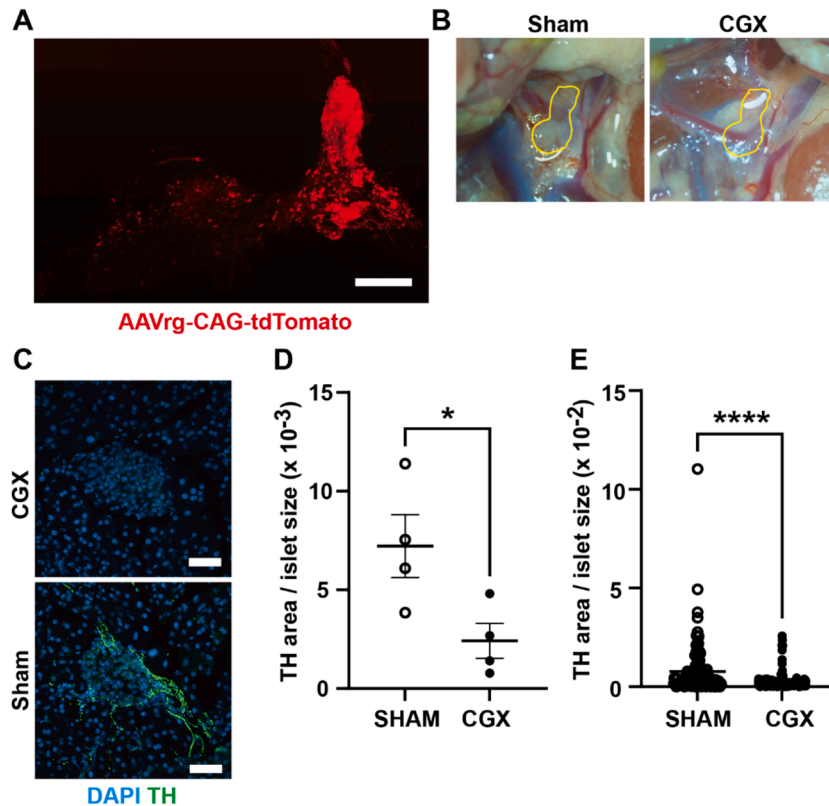


**Fig. 1.** Celiac and superior mesenteric ganglia removal drastically reduces islet sympathetic innervation. (A) Retrograde labeling of celiac and superior mesenteric ganglia (CG-SMG) neurons from the pancreas using AAVrg-CAG-tdTomato. Scale bars, 500  $\mu$ m. (B) Sham and CGX surgery. Yellow lines demonstrate the position of CG-SMG. (C) Immunostaining of anti-tyrosine hydroxylase (TH) (green) and 4',6-diamidino-2-phenylindole (blue) in the islets of sham and CGX group. Scale bars, 50  $\mu$ m. (D) TH area/islet size in each mouse ( $n = 4$  mice each,  $p = 0.038$ ). (E) TH area/islet size of each islet (sham group,  $n = 132$ ; CGX group,  $n = 115$ ;  $p < 0.0001$ ). Data are displayed as means  $\pm$  standard error of the mean. Analyses were performed using the unpaired *t*-test (D) or Mann-Whitney *U* test (E). \* $P < 0.05$ , \*\* $P < 0.01$ , \*\*\* $P < 0.001$ , and \*\*\*\* $P < 0.0001$ .

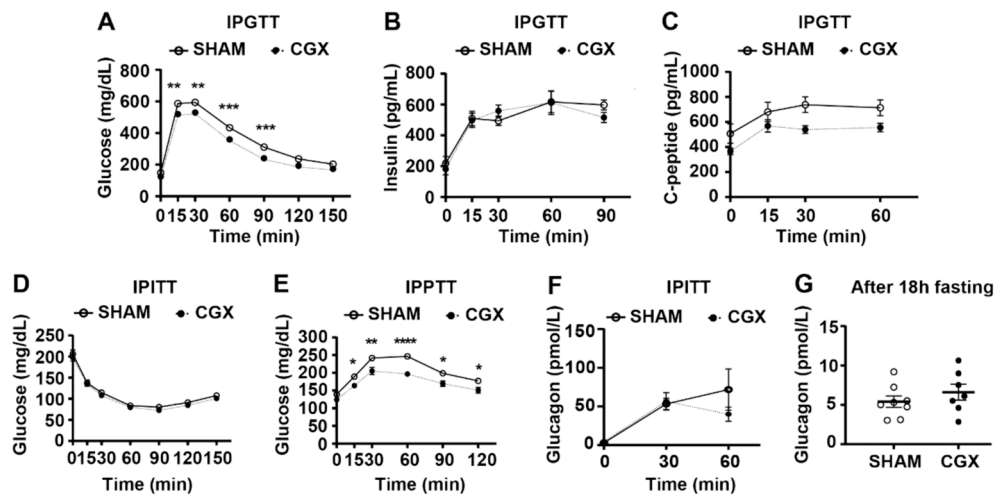


**Fig. 2.** Celiac and superior mesenteric ganglia removal improves glucose tolerance by reducing insulin-dependent gluconeogenesis in the liver. (A) Plasma blood glucose level during intraperitoneal glucose tolerance test (ipGTT) ( $n = 9$  mice each). (B) Plasma insulin level during ipGTT ( $n = 6$  mice each). (C) Plasma C-peptide level during ipGTT ( $n = 7$  mice each). (D) Plasma blood glucose level during intraperitoneal pyruvate tolerance test (ipITT) (sham group,  $n = 7$ ; CGX group,  $n = 8$ ). (E) Plasma blood glucose level during ipPTT ( $n = 8$  mice each). (F) Plasma glucagon level during ipITT (time 0, sham,  $n = 2$ , CGX,  $n = 3$ ; time 30/60,  $n = 4$  mice each). (G) Plasma glucagon level after overnight fasting (sham,  $n = 8$ ; CGX,  $n = 7$ ;  $p = 0.34$ ). Data are shown as means  $\pm$  standard mean of the error. Analyses were performed using a two-way analysis of variance (A, B, C, D, and E), mixed-effects analysis (F), and unpaired  $t$ -test (G). \* $P < 0.05$ , \*\* $P < 0.01$ , \*\*\* $P < 0.001$ , and \*\*\*\* $P < 0.0001$ .

glycogenolysis in the liver.

To explore a possibility that the suppressive effect on insulin release was reduced by CGX, we assessed the changes in circulating insulin and C-peptide levels during ipGTT. C-peptide is a reliable indicator of insulin secretion as it is not cleared by the liver and has a longer half-life than that of insulin (30 min vs. 4 min) [15]. No statistically significant difference in the pre-dose basal levels or post-dose responses of plasma insulin was observed between the sham and CGX groups (Fig. 2B). C-peptide levels appeared to be lower in CGX group, though there was no significant difference (Fig. 2C). To assess changes in insulin sensitivity between the sham and CGX groups, we conducted an ipITT after a 2-h fasting period. Pre-dose basal blood glucose levels (0 min) and post-dose reduction responses (15–150 min) did not exhibit any statistically significant difference between the sham and CGX groups (Fig. 2D).

Next, we tested a possibility of changes in liver gluconeogenesis by performing ipPTT after overnight fasting (Fig. 2E). Pre-dose basal blood glucose levels (0 min) demonstrated no statistically significant differences between the sham and CGX groups. After pyruvate injection, blood glucose levels increased in both groups; however, the responses in the CGX group were significantly lower than those in the sham group. These results indicated that CGX-impaired gluconeogenesis in the liver led to an improvement in glucose tolerance.

Glucagon, whose secretion is promoted by sympathetic nerves, counteracts the actions of insulin and addresses hypoglycemia by boosting hepatic glucose output and gluconeogenesis [16,17]. The glucagon test during the ipITT revealed no statistically significant difference in plasma glucagon levels between the sham and CGX groups (Fig. 2F). Consistently, plasma glucagon levels were not altered by CGX treatment (Fig. 2G).

### 3.3. CGX reduces islet size

We compared the size distribution of the islets in each group to determine the reason why insulin release did not change after CGX. In the cumulative plot of islet size, the CGX group exhibited a slight shift towards a smaller islet size compared to that observed in the sham group (Fig. 3A). The islet size fraction also displayed an increase in the small size fraction ( $< 10,000 \mu\text{m}^2$ ) and a reduction in large size fraction ( $> 10,000 \mu\text{m}^2$ ) in CGX groups compared to that in the sham group (Fig. 3B;  $< 500 \mu\text{m}^2$ , 6.82 and 12.17 %;  $500\text{--}5,000 \mu\text{m}^2$ , 34.85 and 31.30

%;  $5000\text{--}10,000 \mu\text{m}^2$ , 18.18 and 23.48 %;  $10,000\text{--}30,000 \mu\text{m}^2$ , 29.55 and 26.96 %;  $> 30,000 \mu\text{m}^2$ , 10.61 and 6.09 %, for sham and CGX, respectively), though it has no statistical significance (Pearson's Chi-squared test,  $p = 0.33$ ). Notably, no significant alteration was detected in total islet density or proportion of islet area in the pancreas following CGX treatment (Fig. 3C and D).

To determine the reason for the size dependency of these changes, we examined the relationship between islet size and sympathetic nerve innervation (Fig. 3E and F). In both groups, islet size and TH-positive area were both largely proportional. Importantly, the reduction in innervation by CGX was especially obvious in large islets.

### 3.4. CGX reduces $\alpha$ and $\beta$ cell area in large islets

Finally, we examined the relationship between  $\alpha/\beta$  cell area and islet size. We identified a reduction in the proportion of  $\beta$  cell area in large islet fractions. In the islet ranging from  $10,000\text{--}30,000 \mu\text{m}^2$ , the insulin area per islet area was two-fold smaller in the CGX group ( $0.17 \pm 0.019$ ) compared to that in the sham group ( $0.083 \pm 0.015$ ) (Fig. 4A and B). Similarly, the  $\alpha$  cell area per islet size was reduced in the islet ranging from  $10,000\text{--}30,000 \mu\text{m}^2$  (sham  $0.069 \pm 0.011$  vs. CGX  $0.031 \pm 0.0068$ ) and  $> 30,000 \mu\text{m}^2$  (sham  $0.043 \pm 0.0079$  vs. CGX  $0.0072 \pm 0.0020$ ) (Fig. 4C and D). These results suggest a functional reduction in the number of large islets. Of note, the proportion of  $\alpha$  and  $\beta$  cell was not changed by the resection, suggesting that the reduction in size occurred similarly in both  $\alpha$  and  $\beta$  cell areas (Fig. 4E and F).

## 4. Discussion

To date, no study has elucidated the correlation between islet size distribution and sympathetic innervation. In this study, we conducted a detailed analysis of the relationship between islet size distribution and sympathetic innervation for the first time. As a result, sympathectomy was revealed to cause changes in size distribution, with a decrease in large islets and an increase in small islets. As no change in density was noted, the large islets were considered simply to not have undergone selective death. Rather, the large islets likely shrank and transitioned to smaller ones, leading to an increase in the proportion of small islets. Cell death in large islets and/or cell proliferation in small islets could be tested using TUNEL and Ki67 staining, respectively, in future studies.

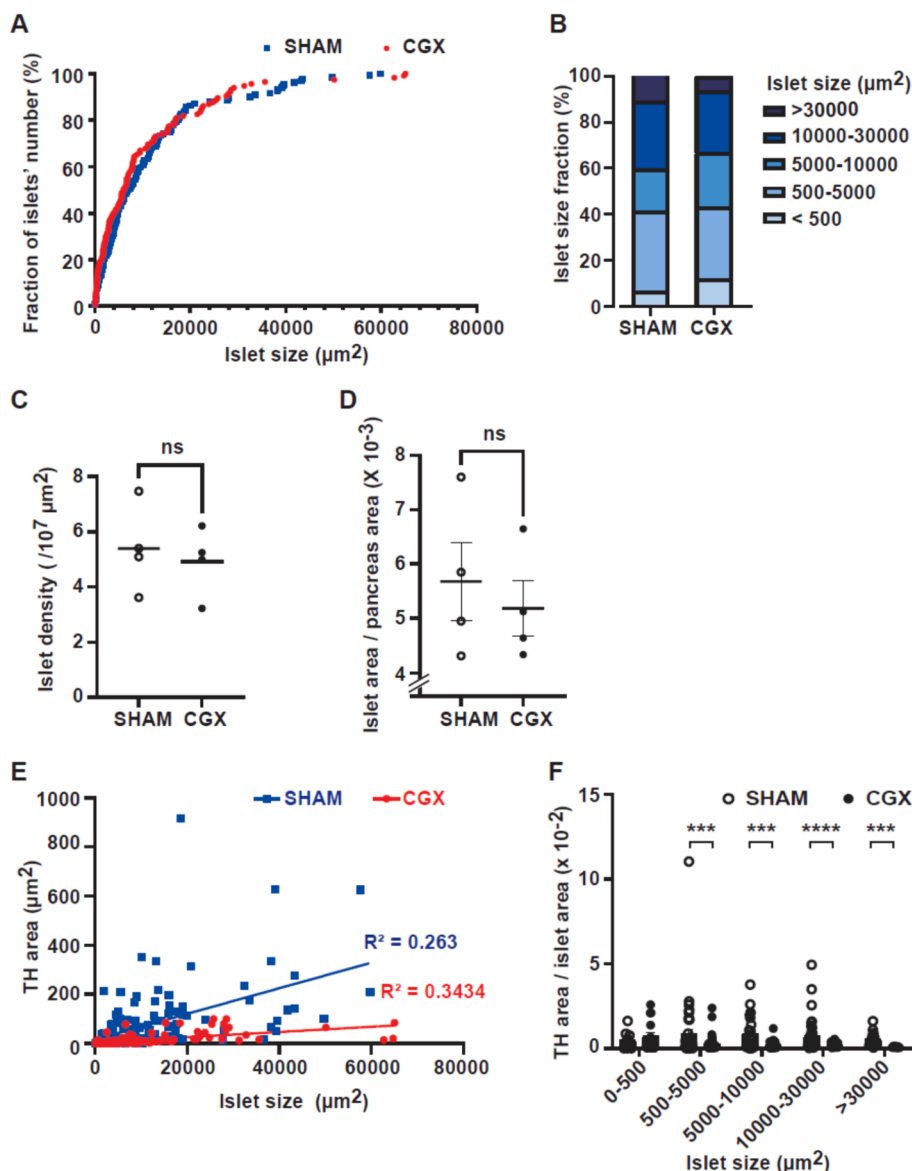


**Fig. 3.** Celiac and superior mesenteric ganglia removal reduces islet size. (A) Cumulative curve of the islet size distribution (sham group,  $n = 132$ ; CGX group,  $n = 115$  from 4 mice each). (B) Percentage of different-size islets. (C) Islet number/pancreas area in each mouse ( $n = 4$  mice each). (D) Islet area/pancreas area in each mouse ( $n = 4$  mice each). (E) Relationship between islet size and anti-tyrosine hydroxylase (TH) area. The formulas of linear regression are  $Y = 0.0052X + 16.60$  (Sham) and  $Y = 0.0011X + 4.23$  (CGX). (F) Relationship between islet size and the ratio of TH area to islet area. Data are demonstrated as means  $\pm$  standard mean of the error. Analyses were performed using the unpaired  $t$ -test (C, D) or Mann-Whitney  $U$  test (F). \* $P < 0.05$ , \*\* $P < 0.01$ , \*\*\* $P < 0.001$ , and \*\*\*\* $P < 0.0001$ .

Previous studies have reported that in certain pathological conditions, large islets are more vulnerable than small islets. In streptozotocin (STZ)-treated rats, the total number of islets decreased, with a particularly notable reduction in large islets (12,501–20,000  $\mu\text{m}^2$ ) and very large islets ( $>20,000 \mu\text{m}^2$ ) [18]. Additionally, in patients with type 2 diabetes, large islets (diameter  $> 60 \mu\text{m}$ ) are preferentially lost compared to those in non-diabetic individuals [19]. However, no compelling explanation exists as to why large islets are lost preferentially. In this study, we revealed for the first time that large islets are significantly susceptible to the loss of sympathetic innervation. This indicates that the attenuation of sympathetic activity due to diabetic neuropathy selectively impacts large islets, elucidating their susceptibility to diabetes.

To determine whether the CGX effects on function vary with islet size, analyzing the secretion of insulin, C-peptide, or glucagon at the level of individual islets in addition to immunohistochemical evaluations is essential. Recent advancements in *in vitro* research techniques

have facilitated the measurement of the insulin secretion profiles of individual islets using methods such as fluorescence anisotropy [20] and electrophoretic immunoassays [21,22]. However, these techniques have not succeeded in reproducing dynamic sympathetic control in the CG *in vitro*. Further technological advancements are required for future research.

The CG/SMG encompasses neurons that regulate multiple organs, including the liver; therefore, CGX can affect various organs. Indeed, improvements in glucose tolerance in Fig. 2A were thought to have originated from changes in liver function. Since C-peptide is less susceptible to degradation compared to insulin, the difference between insulin and C-peptide is considered to reflect the difference in insulin clearance by liver. In Fig. 2C, the C-peptide levels appear lower in CGX, though no reduction was observed in insulin levels. Accordingly, reduction in C-peptide levels may suggest that insulin clearance is slightly reduced in CGX group. This could be due to impaired sympathetic control for the liver function.

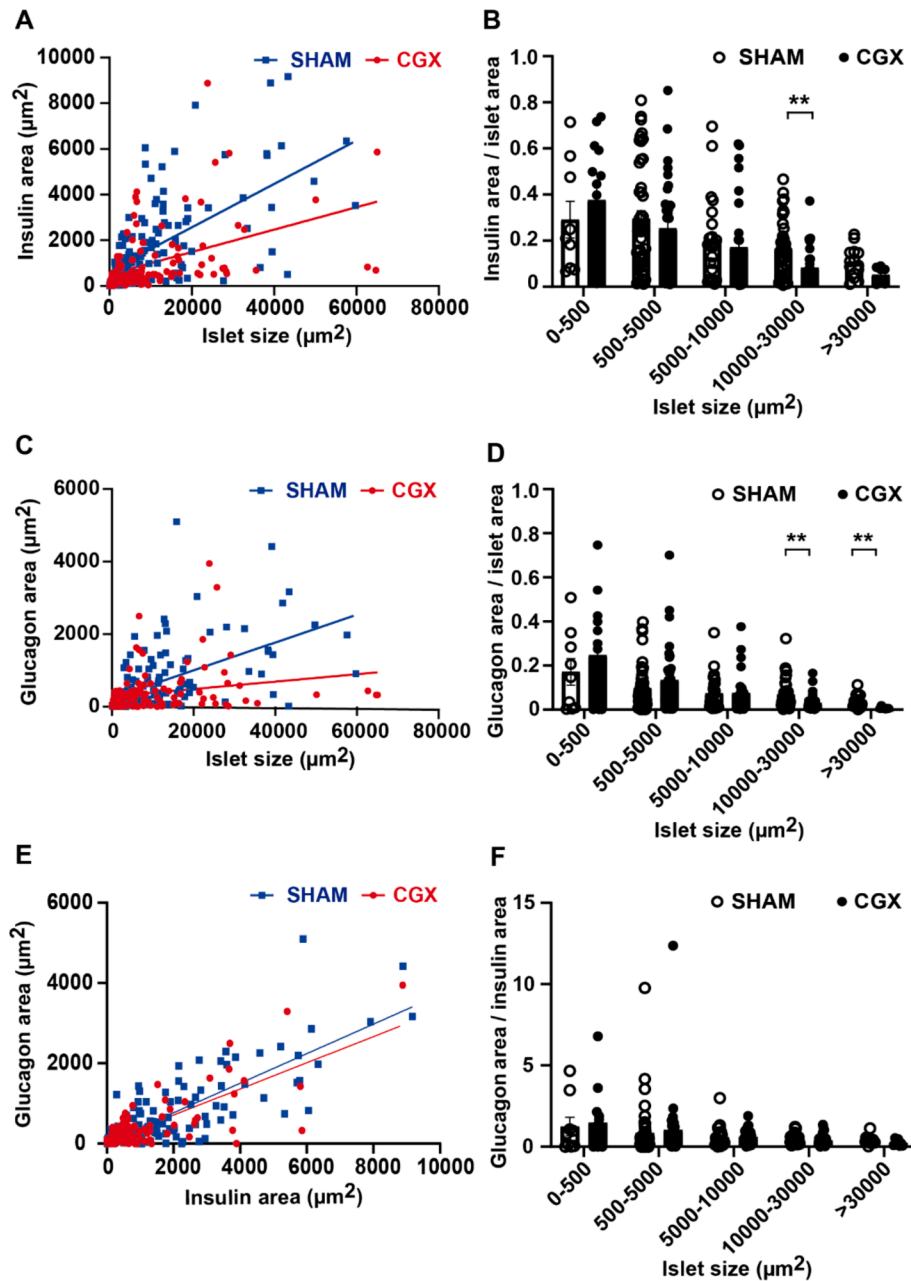


**Fig. 4.** Celiac and superior mesenteric ganglia removal reduces  $\alpha$  and  $\beta$  cell area in large islets. (A) Relationship between islet size and insulin area (sham group,  $n = 132$ ; CGX group,  $n = 115$  from 4 mice each). The formulas of linear regression are  $Y = 0.095X + 666.0$  (Sham) and  $Y = 0.049X + 505.10$  (CGX). (B) Relationship between islet size and the ratio of insulin area to islet area. The formulas of linear regression are  $Y = 0.038X + 237.80$  (Sham) and  $Y = 0.010X + 283.60$  (CGX). (C) Relationship between islet size and glucagon area. The formulas of linear regression are  $Y = 0.038X + 237.80$  (Sham) and  $Y = 0.010X + 283.60$  (CGX). (D) Relationship between islet size and the ratio of glucagon area to islet area. The formulas of linear regression are  $Y = 0.37X + 31.23$  (Sham) and  $Y = 0.33X + 58.54$  (CGX). (E) Relationship between insulin area and glucagon area. The formulas of linear regression are  $Y = 0.37X + 31.23$  (Sham) and  $Y = 0.33X + 58.54$  (CGX). (F) Relationship between islet size and the ratio of glucagon area to insulin area. Data are displayed as means  $\pm$  standard mean of the error. Analyses were performed using the Mann–Whitney  $U$  test (B, D, F). \* $P < 0.05$ , \*\* $P < 0.01$ , \*\*\* $P < 0.001$ , and \*\*\*\* $P < 0.0001$ .

Refuting the possibility that signals from other organs affected by sympathetic nerve deficiency may have influenced the changes in islet size observed in this study is challenging. To address this issue, experiments that selectively control the activity of sympathetic nerves innervating the pancreas are required. Attempts to express proteins in the pancreas by injecting AAV expressing Cre and Cre-dependent AAV into the CG and pancreas, respectively, have revealed limited expression [10]. Further technological improvements will be necessary in the future.

We discovered that CGX resulted in a decrease in the  $\alpha$  and  $\beta$  cell areas only in large islets. A strong correlation between  $\beta$  cell area and

established indicators of  $\beta$  cell function and blood glucose control was reported [23]. In addition, blood glucose control is closely associated with the human pancreatic  $\beta$  cell area [4,24]. In patients with type 2 diabetes, the proportion of  $\beta$  cells in large islets is reduced [19]. Our results suggest that the reduction of the  $\beta$  cells in large islets in diabetes may be caused by a reduction in sympathetic activity. Considering a decrease in  $\beta$  cell mass is implicated in both type 1 and type 2 diabetes (65 % in type 2 diabetes, 99 % in type 1 diabetes) [25–27], further investigation on the long-term sympathetic modulation on  $\beta$  cell size would contribute to the understanding of diabetes pathology and future therapeutic developments.

## 5. Conclusion

In this study, we found that gangliectomy caused a size reduction in larger islets and a decrease in the proportion of  $\alpha$  and  $\beta$  cells within each islet within a few weeks. This is the first study to demonstrate that sympathetic nerve activity plays an important role in maintaining pancreatic islets, providing a new perspective on pancreatic function and glucose metabolism. The results of this study will contribute to elucidating the mechanisms of interaction between the sympathetic nervous system and pancreatic islets and may contribute to the development of treatment strategies for pancreatic-related diseases such as diabetes.

## Funding

This study was supported by MEXT/JSPS KAKENHI (Grant Numbers 18H04055, 21K18269, and 23H00422) and AMED (Grant Number JP23gm1510001).

## CRedit authorship contribution statement

**Shanshan Xu:** Writing – original draft, Investigation, Formal analysis, Data curation. **Misaki Inoue:** Data curation. **Yuki Yoshimura:** Data curation. **Kunio Kondoh:** Validation, Formal analysis. **Keiji Naruse:** Supervision. **Takeshi Y. Hiyama:** Writing – review & editing, Writing – original draft, Visualization, Supervision, Project administration, Investigation, Funding acquisition, Formal analysis, Conceptualization.

## Declaration of competing interest

The authors declare that they have no known competing financial interests or personal relationships that could have appeared to influence the work reported in this paper.

## Data availability

Data will be made available on request.

## Acknowledgements

We thank Dr. Hisashi Noma (The Institute of Statistical Mathematics) for suggestions on statistical analyses and Dr. Edward Boyden (Massachusetts Institute of Technology) for AAV-CAG-tdTomato. We also thank the Tottori Bio Frontier, which managed by Tottori prefecture in Japan, for use of research equipment. This study was supported by MEXT/JSPS KAKENHI (Grant Numbers 18H04055, 21 K18269, and 23H00422) and AMED (Grant Number JP23gm1510001).

## References

- [1] R. Candal, V. Reddy, N.S. Samra, Anatomy, Abdomen and Pelvis: Celiac Ganglia, in: StatPearls [Internet], StatPearls Publishing, 2023.
- [2] X.H. Chen, M. Itoh, W. Sun, T. Miki, Y. Takeuchi, Localization of sympathetic and parasympathetic neurons innervating pancreas and spleen in the cat, *J. Auton. Nerv. Syst.* 59 (1996) 12–16.
- [3] H. Torres, C. Huesing, D.H. Burk, A.J.R. Molinas, W.L. Neuhuber, H.R. Berthoud, H. Münzberg, A.V. Derbenev, A. Zsombok, Sympathetic innervation of the mouse kidney and liver arising from prevertebral ganglia, *Am. J. Physiol. – Regul. Integr. Comp. Physiol.* 321 (2021) R328–R337.
- [4] A. Alvarsson, M. Jimenez-Gonzalez, R. Li, C. Rosselot, N. Tzavaras, Z. Wu, A. F. Stewart, A. Garcia-Ocaña, S.A. Stanley, A 3D atlas of the dynamic and regional variation of pancreatic innervation in diabetes, *Sci. Adv.* 6 (2020).
- [5] M. Campbell-Thompson, E.A. Butterworth, J.L. Boatwright, M.A. Nair, L.H. Nasif, K. Nasif, A.Y. Revell, A. Riva, C.E. Mathews, I.C. Gerling, D.A. Schatz, M. A. Atkinson, Islet sympathetic innervation and islet neuropathology in patients with type 1 diabetes, *Sci. Rep.* 11 (2021) 6562.
- [6] Y.-C. Chiu, T.-E. Hua, Y.-Y. Fu, P.J. Pasricha, S.-C. Tang, 3-D imaging and illustration of the perfusive mouse islet sympathetic innervation and its remodelling in injury, *Diabetologia* 55 (2012) 3252–3261.
- [7] R.F. Hampton, M. Jimenez-Gonzalez, S.A. Stanley, Unravelling innervation of pancreatic islets, *Diabetologia* 65 (2022) 1069–1084.
- [8] N.J. Wewer Albrechtsen, J.J. Holst, A.D. Cherrington, B. Finan, L.L. Gluud, E. D. Dean, J.E. Campbell, S.R. Bloom, T.-M. Tan, F.K. Knop, T.D. Müller, 100 years of glucagon and 100 more, *Diabetologia* 66 (2023) 1378–1394.
- [9] L. Norton, C. Shannon, A. Gastaldelli, R.A. DeFronzo, Insulin: The master regulator of glucose metabolism, *Metabolism* 129 (2022) 155142.
- [10] M. Jimenez-Gonzalez, R. Li, L.E. Pomeranz, A. Alvarsson, R. Marongiu, R. F. Hampton, M.G. Kaplitt, R.C. Vasavada, G.J. Schwartz, S.A. Stanley, Mapping and targeted viral activation of pancreatic nerves in mice reveal their roles in the regulation of glucose metabolism, *Nat. Biomed. Eng.* 6 (2022) 1298–1316.
- [11] S. Kawai, Y. Takagi, S. Kaneko, T. Kurosawa, Effect of Three Types of Mixed Anesthetic Agents Alternate to Ketamine in Mice, *Exp. Anim.* 60 (2011) 481–487.
- [12] M. Li, J. Galligan, D. Wang, G. Fink, The effects of celiac ganglionectomy on sympathetic innervation to the splanchnic organs in the rat, *Auton. Neurosci.* 154 (2010) 66–73.
- [13] T.Y. Hiyama, S. Matsuda, A. Fujikawa, M. Matsumoto, E. Watanabe, H. Kajiwara, F. Niimura, M. Noda, Autoimmunity to the sodium-level sensor in the brain causes essential hyponatremia, *Neuron* 66 (2010) 508–522.
- [14] S. Persson-Sjögren, S. Forsgren, I.B. Täljedal, Tyrosine hydroxylase in mouse pancreatic islet cells, in situ and after syngeneic transplantation to kidney, *Histol. Histopathol.* 17 (2002) 113–121.
- [15] J.P. Palmer, G.A. Fleming, C.J. Greenbaum, K.C. Herold, L.D. Jansa, H. Kolb, J. M. Lachin, K.S. Polonsky, P. Pozzilli, J.S. Skyler, M.W. Steffes, C-peptide is the appropriate outcome measure for type 1 diabetes clinical trials to preserve beta-cell function: report of an ADA workshop, 21–22 October 2001, *Diabetes* 53 (2004) 250–264.
- [16] J.H. Exton, L.S.J. Jefferson, R.W. Butcher, C.R. Park, Gluconeogenesis in the perfused liver. The effects of fasting, alloxan diabetes, glucagon, epinephrine, adenosine 3',5'-monophosphate and insulin, *Am. J. Med.* 40 (1966) 709–715.
- [17] R.H. Unger, L. Orci, Role of glucagon in diabetes, *Arch. Intern. Med.* 137 (1977) 482–491.
- [18] O.R. Oyenihi, M.E. Cerf, M.G. Matsabisa, N.L. Brooks, O.O. Oguntibeju, Effect of kolaviron on islet dynamics in diabetic rats, Saudi, *J. Biol. Sci.* 29 (2022) 324–330.
- [19] G. Kilimnik, B. Zhao, J. Jo, V. Periwal, P. Witkowski, R. Misawa, M. Hara, Altered islet composition and disproportionate loss of large islets in patients with type 2 diabetes, *PLoS One* 6 (2011) e27445.
- [20] A.L. Gliberman, B.D. Pope, J.F. Zimmerman, Q. Liu, J.P. Ferrier, J.H.R. Kenty, A. M. Schrell, N. Mukhitov, K.L. Shores, A.B. Tepole, D.A. Melton, M.G. Roper, K. K. Parker, Synchronized stimulation and continuous insulin sensing in a microfluidic human islet on a chip designed for scalable manufacturing, *Lab Chip* 19 (2019) 2993–3010.
- [21] J.F. Dishinger, R.T. Kennedy, Serial Immunoassays in Parallel on a Microfluidic Chip for Monitoring Hormone Secretion from Living Cells, *Anal. Chem.* 79 (2007) 947–954.
- [22] J.F. Dishinger, K.R. Reid, R.T. Kennedy, Quantitative Monitoring of Insulin Secretion from Single Islets of Langerhans in Parallel on a Microfluidic Chip, *Anal. Chem.* 81 (2009) 3119–3127.
- [23] J.J. Meier, B.A. Menge, T.G.K. Breuer, C.A. Müller, A. Tannapfel, W. Uhl, W. E. Schmidt, H. Schrader, Functional assessment of pancreatic  $\beta$ -cell area in humans, *Diabetes* 58 (2009) 1595–1603.
- [24] J.L. Leahy, Natural history of beta-cell dysfunction in NIDDM, *Diabetes Care* 13 (1990) 992–1010.
- [25] A.E. Butler, J. Janson, S. Bonner-Weir, R. Ritzel, R.A. Rizza, P.C. Butler, Beta-cell deficit and increased beta-cell apoptosis in humans with type 2 diabetes, *Diabetes* 52 (2003) 102–110.
- [26] W. Gepts, Pathologic anatomy of the pancreas in juvenile diabetes mellitus, *Diabetes* 14 (1965) 619–633.
- [27] J.J. Meier, A. Bhushan, A.E. Butler, R.A. Rizza, P.C. Butler, Sustained beta cell apoptosis in patients with long-standing type 1 diabetes: indirect evidence for islet regeneration? *Diabetologia* 48 (2005) 2221–2228.